

Fate of Glycosylphosphatidylinositol (GPI)-Less Procyclin and Characterization of Sialylated Non-GPI-Anchored Surface Coat Molecules of Procyclic-Form *Trypanosoma brucei*^{∇†‡}

Maria Lucia Sampaio Güther,¹ Kenneth Beattie,² Douglas J. Lamont,² John James,³
Alan R. Prescott,⁴ and Michael A. J. Ferguson^{1*}

Division of Biological Chemistry and Drug Discovery,¹ FingerPrints Proteomics Facility,² Centre for High-Resolution Imaging,³ and Division of Cell Biology and Immunology,⁴ College of Life Sciences, University of Dundee, Dundee DD1 5EH, United Kingdom

Received 21 June 2009/Accepted 29 June 2009

A *Trypanosoma brucei* TbGPI12 null mutant that is unable to express cell surface procyclins and free glycosylphosphatidylinositols (GPI) revealed that these are not the only surface coat molecules of the procyclic life cycle stage. Here, we show that non-GPI-anchored procyclins are N-glycosylated, accumulate in the lysosome, and appear as proteolytic fragments in the medium. We also show, using lectin agglutination and galactose oxidase-NaB³H₄ labeling, that the cell surface of the TbGPI12 null parasites contains glycoconjugates that terminate in sialic acid linked to galactose. Following desialylation, a high-apparent-molecular-weight glycoconjugate fraction was purified by ricin affinity chromatography and gel filtration and shown to contain mannose, galactose, N-acetylglucosamine, and fucose. The latter has not been previously reported in *T. brucei* glycoproteins. A proteomic analysis of this fraction revealed a mixture of polytopic transmembrane proteins, including P-type ATPase and vacuolar proton-translocating pyrophosphatase. Immunolocalization studies showed that both could be labeled on the surfaces of wild-type and TbGPI12 null cells. Neither galactose oxidase-NaB³H₄ labeling of the non-GPI-anchored surface glycoconjugates nor immunogold labeling of the P-type ATPase was affected by the presence of procyclins in the wild-type cells, suggesting that the procyclins do not, by themselves, form a macromolecular barrier.

The tsetse fly-transmitted protozoan parasite *Trypanosoma brucei* causes human sleeping sickness and the cattle disease Nagana in sub-Saharan Africa. The organism undergoes a complex life cycle between the mammalian host and the insect, tsetse, vector. The bloodstream form of the parasite expresses a dense monolayer of glycosylphosphatidylinositol (GPI)-anchored variant surface glycoprotein dimers and avoids specific immune responses through antigenic variation (32, 47). Following ingestion in a blood meal, the parasites differentiate into procyclic-form parasites that colonize the tsetse midgut. The procyclic trypanosomes express a radically different cell surface coat that includes about 3×10^6 procyclin glycoproteins (28, 36, 37) and about 1×10^6 poly-N-acetyllactosamine-containing free GPIs (19, 29, 39, 55). The procyclins are polyanionic, rod-like (38, 50) proteins encoded by procyclin genes. In *T. brucei* strain DD1 5EH, used in this study, the parasites contain (per diploid genome) two copies of the *GPEET1* gene, encoding 6 Gly-Pro-Glu-Glu-Thr repeats; one copy each of the *EP1-1* and *EP1-2* genes, encoding EP1 procyclins with 30 and 25 Glu-Pro repeats, respectively; two copies of the *EP2-1* gene, encoding EP2 procyclin with 25 Glu-Pro repeats; and two copies of the *EP3-1* gene, encoding EP3 procyclin with 22

Glu-Pro repeats (1). The EP1 and EP3 procyclins contain a single N-glycosylation site, occupied exclusively by a conventional Man₅GlcNAc₂ oligosaccharide, at the N-terminal side of the Glu-Pro repeat domain (1, 50). Whereas neither EP2 nor GPEET procyclin is N-glycosylated, GPEET1 procyclin is phosphorylated on six out of seven Thr residues (25). In culture, the procyclin expression profile depends on the carbon source (56) and metabolic state of the cells (27), and in the tsetse fly, there appears to be a program of procyclin expression such that GPEET procyclin is expressed early, giving way to EP1 and EP3 procyclin expression (2, 54). GPEET and EP procyclins contain similar GPI membrane anchors. These are based on the ubiquitous ethanolamine-*P*-6Man α 1-2Man α 1-6Man α 1-4GlcNAc α 1-6PI core (where, in this case, the PI lipid is a 2-*O*-acyl-*myo*-inositol-1-*P*-*sn*-2-*lyso*-1-*O*-acylglycerol structure [50]), but they also contain the largest and most complex known GPI side chains. These side chains are large poly-disperse-branched poly-N-acetyllactosamine structures (with an average of about 8 to 12 repeats, depending on the preparation) that can terminate with α 2- and α 3-linked sialic acid residues (9, 50). Sialic acid is transferred from serum sialoglycoconjugates to terminal β -galactosidase residues by the action of a cell surface GPI-anchored *trans*-sialidase enzyme (7, 26, 34). The *trans*-sialylation of surface components plays a role in the successful colonization of the tsetse fly (29). In vivo, the N termini of the procyclins are removed by tsetse fly gut proteases (2), though the role of this event is unclear (20) and it is thought that the underlying (protease-resistant) anionic repeat units and associated GPI anchor side chains might protect the parasite from the approach of tsetse fly gut hydrolases (2).

The cell surface architecture of procyclic trypanosomes has

* Corresponding author. Mailing address: Division of Biological Chemistry and Drug Discovery, College of Life Sciences, University of Dundee, Dundee DD1 5EH, United Kingdom. Phone: 44-1382 384219. E-mail: m.a.j.ferguson@dundee.ac.uk.

† Supplemental material for this article may be found at <http://ec.asm.org/>.

[∇] Published ahead of print on 24 July 2009.

[‡] The authors have paid a fee to allow immediate free access to this article.

been manipulated by the gene knockout of the procyclin genes themselves (55, 57), by galactose starvation (39), and by the knockout or knockdown of genes encoding enzymes of the GPI biosynthetic pathway, i.e., TbGPI10, TbGPI8, and TbGPI12 (11, 19, 29, 30). The procyclin TbGPI10 and TbGPI8 knockouts all resulted in parasites devoid of GPI-anchored procyclins, but this was compensated for by an upregulation in free GPI expression. However, the TbGPI12 null mutants that cannot synthesize GPI structures beyond GlcNAc-PI, revealed the presence of previously unidentified non-GPI-anchored surface coat components. In this paper, we characterize the fate of non-GPI-anchored procyclin protein and characterize the non-GPI-anchored surface coat components.

MATERIALS AND METHODS

Cultivation of procyclic-form trypanosomes. Procyclic *T. brucei* strain 427 clone 29.13 cells, referred to as wild-type cells, were cultured at 28°C in SDM-79 in the presence of 15% fetal bovine serum, 2 mM Glutamax (Invitrogen), and 7.5 mg/liter hemin (5) containing 15 µg/ml G418 and 50 µg/ml hygromycin. The creation of the TbGPI12 null cells and the culture conditions were described previously (11). Large cultures of the TbGPI12 null cells were prepared as described above using roller bottles and gently rotated for 2 to 3 days.

Biosynthetic labeling of TbGPI12 null cells with radioactive sugars and [¹⁴C]proline. Washed wild-type and TbGPI12 null cells (5 ml at 10⁷ cells/ml) were labeled with [³H]glucosamine, [³H]mannose, and [³H]glucose in glucose-free SDM-79 containing 2% dialyzed fetal bovine serum. For the [¹⁴C]proline labeling, SDM-79 was depleted of L-proline and hydroxyproline. The labeling was performed using 50 µCi/ml of sugar radioisotopes for 3 h, or using 10 µCi/ml of [¹⁴C]proline for 2 and 20 h, at 28°C. The labeled cells were washed in ice-cold phosphate-buffered saline (PBS), resuspended in 15 µl PBS, and boiled with an equal volume of 2× concentrated sodium dodecyl sulfate (SDS)-sample buffer containing 0.2 M dithiothreitol (DTT). The [¹⁴C]proline-labeling culture supernatant was centrifuged, filtered (0.2-µm pore size), and immunoprecipitated for 2 h at 4°C with 5 µg anti-EP procyclin antibody (Cedarlane Laboratories, Canada) and 20 µg protein G-agarose (Pierce). The beads were washed in PBS containing 0.1% SDS and 1% Triton X-100 (TX-100), boiled in SDS-sample buffer containing 0.1 M DTT, and run on 12% or 4 to 12% Nupage/MOPS (morpholinepropanesulfonic acid) gels (Invitrogen). For the experiment for which the results are shown in Fig. 3D, total cells labeled with [³H]mannose were boiled in SDS-sample buffer with 0.1 M DTT, diluted to 0.03% SDS with 1% TX-100 in 20 mM Tris-HCl (pH 7.2) and 0.15 M NaCl, and pulled down with 30 µl ricin-agarose (Vector Labs) for 2 h at 4°C. The beads were washed in 0.03% SDS and 1% TX-100 buffer, boiled in SDS-sample buffer with 0.1 M DTT, and applied to a 4 to 12% Nupage gel. The gels were impregnated with En³Hance (Perkin-Elmer), dried, and taken for fluorography at -80°C with an intensifying screen.

Galactose oxidase-sodium borotritide labeling of live procyclic cells. Procyclic cells (2 × 10⁷) were washed, resuspended in 1 ml SDM-79 minus fetal bovine serum containing 1 mM nonradioactive NaBH₄ (to block reducible sites), and incubated with 5 mU/ml of *Clostridium perfringens* neuraminidase (Sigma) for 30 min at 28°C. The cells were washed and resuspended in PBS and incubated with 1.5 U/ml of *Dactylium dendroides* galactose oxidase (Sigma) (previously heated for 30 min at 50°C to destroy protease contaminant activity) for 30 min at 37°C. The cells were washed, resuspended in 0.5 ml PBS, and labeled for 30 min at 28°C with 2 µl of 0.4 Ci/ml NaB[³H]₄ (Perkin Elmer) dissolved in 0.1 M NaOH. The cell pellet was resuspended in 1 mM freshly prepared nonradioactive NaBH₄ in PBS, washed three times in PBS, boiled in SDS-sample buffer containing DTT, loaded onto 4 to 12% Nupage/MOPS gels (Invitrogen), and processed for fluorography as described above.

Lectin agglutination experiments. Wild-type and TbGPI12 null cells were washed, resuspended at 2 × 10⁷ cells/ml in SDM-79 medium minus fetal bovine serum, and incubated for 1 h at 28°C with an equal volume of 0.2 µg/ml lectin (Vector Labs, United Kingdom) before examination by light microscopy under phase contrast. Lectin final concentrations of 0, 1, 2.5, and 10 µg/ml were also tested (data not shown). Pretreatment with 0.2 mU of *Clostridium perfringens* neuraminidase (Roche) was performed for 30 min at 28°C in SDM-79 medium minus fetal bovine serum.

High-MW glycoconjugate purification by ricin-agarose and gel filtration. TbGPI12 null cells (5 liters at about 4 × 10⁷ cells/ml) were harvested by centrifugation at 600 × g for 10 min at 4°C, washed with PBS, and hypotonically

lysed in water containing 0.1 mM TLCK (*N*- α -tosyl-L-lysine chloromethyl ketone), 2 µg/ml leupeptin, 1 mM phenylmethylsulfonyl fluoride, and 1 µg/ml aprotinin. The cell ghosts were recovered by centrifugation at 13,000 × g for 10 min at 4°C and washed three times with 100 ml ice-cold 20 mM Tris-HCl (pH 6.8), 0.15 M NaCl. The final cell ghost pellet was extracted with SDS-urea and purified on ricin-agarose beads (RCA120-agarose; Vector Labs, United Kingdom) as described previously (3). The beads (10-ml packed volume) were packed into a column, washed with 100 ml wash buffer (0.06% SDS, 0.8% *n*-octylglucoside, 0.1 M DTT, 20 mM Tris-HCl [pH 6.8], 0.2 M NaCl, 0.05% sodium azide), and eluted with 17 ml of 30 mg/ml of each galactose and lactose in wash buffer at 4°C. The beads were further eluted at 50°C with 10 ml 1% SDS, 0.1 M DTT, 20 mM Tris-HCl (pH 6.8), 0.2 M NaCl, 30 mg/ml galactose, and 30 mg/ml lactose and at 100°C with 10 ml of the same buffer. The combined eluates were diluted to a final concentration of 0.1% SDS, concentrated to 1 ml using a Vivaspin 20 concentrator (Sartorius) and loaded onto a Superose 6B gel filtration column (1 by 30 cm; GE Healthcare) at 0.5 ml/min using 20 mM Tris-HCl (pH 6.8) containing 0.15 M NaCl, 0.1% (wt/vol) SDS, 10 mM DTT. Fractions (0.5 ml) were collected, applied on 4 to 12% Nupage/MOPS gels, and stained or blotted to nitrocellulose as described below. Superose 6B molecular weight (MW) calibration curves were performed using 0.5 mg of each blue dextran, thyroglobulin, apoferritin, β -amylase, and bovine serum albumin (BSA).

Proteomics. An aliquot of fraction 18 from Superose chromatography was reduced and alkylated with iodoacetamide in SDS-sample buffer, run on 4 to 12% Nupage/MOPS gels, and stained with colloidal Coomassie blue (Simply Blue; Invitrogen). The center of the band was excised and subjected to in-gel digestion with trypsin. The resulting peptides were analyzed, in the Dundee University Fingerprints Proteomics Facility, by liquid chromatography-tandem mass spectrometry (LC-MS/MS) on a Thermo Finnigan Orbitrap instrument equipped with a Dionex 3000 nano-LC. The data were processed by Mascot.

Immunofluorescence and transmission electron microscopy. *T. brucei* procyclic-form cultures (2 × 10⁷ cells/ml) were harvested by centrifugation at 600 × g, washed in ice-cold PBS, fixed on coverslips with 4% paraformaldehyde in PBS for 15 min at room temperature (RT), permeabilized in 0.05% TX-100 in PBS, and blocked with 1% (vol/vol) fish-skin gelatin (Sigma) in PBS. For the experiment for which the results are shown in Fig. 1, the samples were double labeled for 1 h at RT with 1:2,000 mouse monoclonal anti-EP procyclin (Cedarlane, Canada) and 1:250 rabbit polyclonal anti-trypanopain (kind gift of Jay BANGS, Madison, WI). Subsequently, they were washed in fish-skin gelatin in PBS, incubated for 1 h at RT with a mix of 1:500 of anti-mouse Alexa Fluor 468 (green) and 1:500 anti-rabbit Alexa Fluor 588 (red) (Molecular Probes). The coverslips were further washed and mounted onto slides using Hydromount (National Diagnostics) containing 2.5% (wt/vol) Dabco (Sigma) and visualized with a Zeiss 510 microscope. For the experiment for which the results are shown in Fig. 7A, the coverslips containing fixed wild-type and TbGPI12 null procyclic cells were incubated with 1:400 rabbit polyclonal anti-P-type ATPase (kind gift of Roberto Docampo, University of Georgia). For the experiment for which the results are shown in Fig. 7B, live parasites were incubated for 1 h at 4°C with 1:400 rabbit polyclonal anti-vacuolar-type proton pyrophosphatase (VHPPase) (a kind gift of Norbert Bakalara, ENSCM, France) or 1:400 rabbit polyclonal anti-VHPPase peptides 324 and 326 raised against *Arabidopsis thaliana* VHP-Pase putative hydrophilic loops IV and XII, respectively (kind gift of Philip Rea, University of Pennsylvania, Philadelphia, PA). Subsequently, the parasites were washed and fixed on coverslips with 4% paraformaldehyde in PBS. The secondary antibody was 1:500 anti-rabbit Alexa Fluor 468, which was mounted and visualized as described above.

For the transmission electron microscopy for which the results are shown in Fig. 8, in vivo single labeling was performed prior to fixation and cryosectioning. Wild-type and TbGPI12 null procyclic cells (10⁷ parasites in 0.5 ml SDM-79 plus 15% fetal bovine serum) were incubated for 1 h at 4°C with 1:10 rabbit polyclonal anti-P-type ATPase. The cells were washed with cold medium, resuspended, and fixed for 15 min in 4% (wt/vol) paraformaldehyde in PBS. The cells were washed in PBS and incubated with 1:50 protein A-10-nm gold (BBInternational, Cardiff, United Kingdom) for 30 min at 28°C. The cells were washed and resuspended in 0.5 ml PBS and fixed by adding 0.5 ml of 5% (vol/vol) glutaraldehyde containing 2% (wt/vol) tannic acid (Sigma) in 0.2 M cacodylate-HCl (pH 6.9). The cells were washed in 0.1 M cacodylate-HCl (pH 6.9), fixed for 1 h in 1% OsO₄ containing 1.5% sodium ferrocyanide in cacodylate buffer, dehydrated in ethanol, and embedded in Durcupan overnight. Ultrathin sections were stained with 3% aqueous uranyl acetate, followed by Reynolds lead citrate, and imaged on an FEI (Eindhoven, The Netherlands) Tecnai 12 transmission electron microscope. The images collected on digital imaging plates were scanned on a DITABIS micron scanner (Pforzheim, Germany).

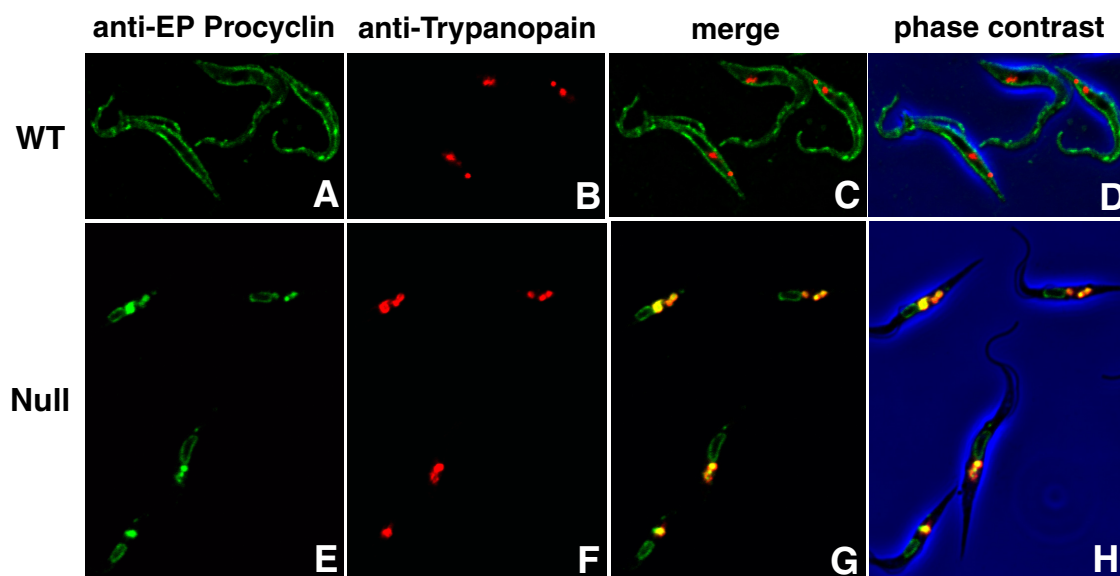


FIG. 1. Procyclin localizes predominantly to the lysosomes in TbGPI12 null cells. Immunofluorescence microscopy of wild-type (WT) and TbGPI12 null (Null) procyclic trypanosomes stained with anti-EP procyclin (panels A and E; the TbGPI12 null mutant and its wild-type parent cell line express almost exclusively EP procyclins [25]) and anti-trypanopain (panels B and F) antibodies, as indicated. The merged images (panels C and G) and merged images together with the corresponding phase-contrast images (panels D and H) are also shown. Trypanopain is a lysosomal marker (51).

Reducing SDS-polyacrylamide gel electrophoresis (PAGE) and Western blotting. Superose 6B fractions were run on reducing 4 to 12% Nupage/MOPS gels and either stained with Coomassie blue (Simply Blue; Invitrogen) or periodate-Schiff reagent (Sigma) or, alternatively, transferred onto nitrocellulose and blocked with blocking buffer (0.5% [wt/vol] BSA, 0.05% [wt/vol] NP-40 [Igepal; Sigma], 50 mM Tris-HCl [pH 7.4]). In the experiment for which the results are shown in Fig. 5, nitrocellulose was probed with 1:2,000 biotinylated ricin, followed by washes in blocking buffer, incubation with 1:10,000 Extravidin horseradish peroxidase (Sigma), and detection with ECL reagents (GE Healthcare). In the experiment for which the results are depicted in Fig. 6, nitrocellulose was probed with 1:400 anti-P-type ATPase or 1:400 anti-VHPPase (a kind gift from Norbert Bakalara) diluted in blocking buffer. After washing in blocking buffer, the blots were incubated with 1:5,000 goat anti-rabbit antibodies conjugated to horseradish peroxidase (Stratech, United Kingdom) and detected by ECL.

Sugar composition analysis by GC-MS. Superose 6 fraction 18 was desalted by diafiltration using a Microcon 30 (Amicon) concentrator. Aliquots were subsequently mixed with 2 nmol of a *scyllo*-inositol internal standard and subjected to acid methanolysis, re-N-acetylation, and trimethylsilylation, and the derivatives were analyzed and quantified by GC-MS, as described previously (3, 8). The monosaccharide quantifications were compared to total protein measured by the bicinchoninic acid method (Pierce) using BSA as the standard.

RESULTS

Fate of non-GPI-anchored procyclin in TbGPI12 null cells.

Procyclin was localized by immunofluorescence microscopy using anti-EP procyclin antibodies in wild-type (Fig. 1A) and TbGPI12 null cells (Fig. 1E). The former gave the expected cell surface labeling, whereas the latter produced a weak perinuclear pattern together with a strong punctate stain between the nucleus and the flagellar pocket, reminiscent of a lysosomal location. To assess this, the cells were also stained with antibodies to a lysosomal marker protein, trypanopain (33, 51). In the wild-type cells, there was no significant colocalization (Fig. 1B to D), whereas in the TbGPI12 null cells, there was considerable colocalization of the procyclin and trypanopain signals (Fig. 1F to H). These data suggest that, in the absence of

GPI anchoring, the procyclins are found partly in the endoplasmic reticulum (ER) and mostly in the lysosomes.

To further investigate the fate of procyclin, wild-type and TbGPI12 null cells were metabolically labeled with [14 C]proline for 2 h and 20 h at 28°C. Subsequently, cell lysates and their respective culture supernatants were immunoprecipitated with anti-EP procyclin antibodies and protein G-agarose. The immunoprecipitates were analyzed by liquid scintillation counting (Table 1) and by SDS-PAGE and fluorography (Fig. 2). The wild-type cells showed the usual diffuse band (apparent molecular mass, 32 to 45 kDa) of fully processed procyclin at both 2 and 20 h of labeling (Fig. 2A, lanes 1 and 2), and a small proportion (16%) (Table 1) of the label at 20 h was found in the supernatant (Fig. 2A, lane 4).

The TbGPI12 null cell lysates showed labeled bands of apparent molecular masses of 29, 27, and 26 kDa (Fig. 2A, lanes 5 and 6), and by 20 h, 55% (Table 1) of the label was found in the culture supernatant in the form of multiple bands, ranging

TABLE 1. Distribution of cellular and shed or secreted [14 C]proline-labeled EP procyclin in wild-type and TbGPI12 null cells

Labeling (h)	WT cpm (% total cpm)		TbGPI12 null cpm (% total cpm)	
	Cell lysate	Culture supernatant	Cell lysate	Culture supernatant
2	14,000 (98)	300 (2)	18,000 (97)	500 (3)
20	89,000 (84)	17,000 (16)	105,000 (45)	130,000 (55)

^a Wild-type (WT) and TbGPI12 null procyclic trypanosomes were labeled with [14 C]proline for 2 or 20 h, and their cell lysates and corresponding culture supernatants were immunoprecipitated with anti-EP procyclin antibodies. Aliquots were taken for liquid scintillation counting.

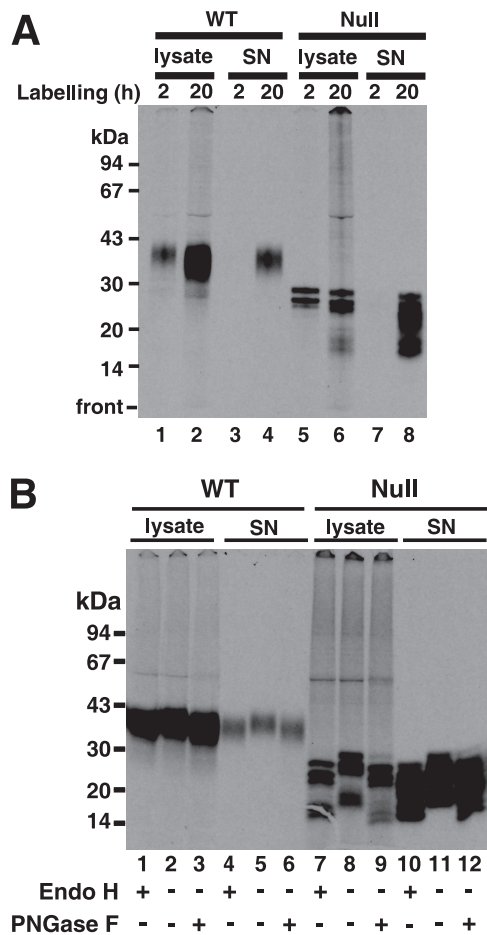


FIG. 2. Procyclin is N-glycosylated, proteolytically processed, and secreted from TbGPI12 null cells. (A) Wild-type (WT) cells (lanes 1 to 4) and TbGPI12 null (Null) cells (lanes 5 to 8) were labeled with [^{14}C]proline for 2 and 20 h, and their corresponding cell lysates and culture supernatants (SN) were immunoprecipitated with anti-EP antibody and analyzed by SDS-PAGE and fluorography. (B) Samples from the 20-h labeling were digested with and without endo H and PNGase F, as indicated, and analyzed by SDS-PAGE and fluorography. The positions of the MW markers are shown on the left.

in apparent molecular masses from 27 to 17 kDa. The digestion of the 20-h samples with endoglycosidase H (endo H) and peptide N-glycosidase F (PNGase F) showed that every band was susceptible to both enzymes (Fig. 2B). From these data, we can conclude that all of the procyclin fragments observed in the TbGPI12 null sample are N-glycosylated with oligomannose structures.

Additional [^{14}C]proline-labeling experiments using the cysteine protease inhibitor FMK24, known to inhibit the lysosomal cysteine proteases of *T. brucei* (51), were performed. The presence of this compound reduced the formation of low-MW procyclin fragments in the TbGPI12 null cells (see Fig. S1 in the supplemental material), supporting the view that procyclin degradation occurs, at least in part, in the lysosome.

Biosynthetic labeling of TbGPI12 null cells with radioactive sugars. Previously, we reported that the TbGPI12 null surface coat could be stained with ruthenium red, a glycolyx dye, indicating that procyclic trypanosomes have non-GPI-anchored car-

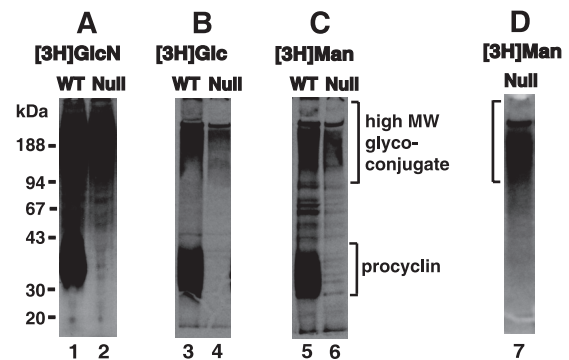


FIG. 3. Radiolabeling of a high-apparent-MW glycoconjugate fraction with ^3H -monosaccharides. Wild-type (WT) and TbGPI12 null (Null) procyclic trypanosomes were biosynthetically labeled with [^3H]glucosamine [$[^3\text{H}]\text{GlcN}$; panel A, lanes 1 and 2], [^3H]glucose [$[^3\text{H}]\text{Glc}$; panel B, lanes 3 and 4] and [^3H]mannose [$[^3\text{H}]\text{Man}$; panel C, lanes 5 and 6], as indicated. Cell lysates were analyzed by SDS-PAGE and fluorography. The lysates of the [^3H]mannose-labeled TbGPI12 null cells were also subjected to a pull-down on ricin-agarose (panel D, lane 7). The positions of the MW markers are shown on the left.

bohydrate-containing surface coat molecules in addition to GPI-anchored procyclins (11). To further characterize the nature of these other surface coat molecules, we labeled wild-type and TbGPI12 null cells with [^3H]mannose and [^3H]glucose and analyzed the labeled samples by SDS-PAGE and fluorography. These data are shown alongside our previously reported [^3H]glucosamine labeling (Fig. 3A). In all cases, we detected a smear of radiolabeled molecules that was present in both the wild-type and TbGPI12 null cells (Fig. 3, lanes 1 to 6). We refer to this labeled material that runs with an apparent molecular mass from 90 kDa to >200 kDa (high-MW glycoconjugate). This material was also labeled with [^3H]serine and [^{35}S]methionine, indicating it contains protein or peptide components (data not shown). In the wild-type cells, all of the sugars also labeled the procyclins, as expected (Fig. 3, lanes 1, 3, and 5).

Interestingly, whereas the cell-associated N-glycosylated [^3H]proline-labeled 29-, 27-, and 26-kDa procyclin fragments are clearly visible after 2 h of labeling (Fig. 2A, lane 5), there is only a very weak signal in those fragments during the 3-h [^3H]mannose-labeling experiment (Fig. 3C, lane 6). We investigated the relative efficiencies of [^3H]mannose incorporation into the GPI anchor and the N-linked oligosaccharide of procyclin by repeating the 3-h [^3H]mannose-labeling experiment with wild-type cells and analyzing the procyclin by SDS-PAGE before and after treatment with PNGase F. The shift in apparent MW confirmed the removal of the N-linked glycan, and the subsequent in-gel base digestion, neutralization, and scintillation counting revealed that 70% of the radioactivity was associated with the GPI anchor, despite it containing only three Man residues compared with five in the N-glycan. The relatively low efficiency of radiolabeling of the N-glycan versus the GPI anchor presumably represents a much longer half-life for steady-state labeling of the $\text{Man}_9\text{GlcNAc}_2\text{-PP-Dol}$ N-glycan precursor than that for the GPI anchor precursor in wild-type cells. This, together with the observed proteolytic turnover of the non-GPI-anchored procyclin in the TbGPI12 null mutant, provides an explanation for the aforementioned discrepancy.

TABLE 2. Agglutination of wild-type (WT) and TbGPI12 null cells by lectins^a

Lectin	Lectin specificity	Neuraminidase pretreatment	Degree of agglutination for indicated cells	
			WT	TbGPI12 null
WGA	GlcNAc/sialic acid	No	+++	+++
	GlcNAc/sialic acid	Yes	-	-
Ricin (RCA 120)	Terminal Gal or GalNAc	No	-	-
	Terminal Gal or GalNAc	Yes	+++	+++
Concanavalin A	α-Mannose	No	+++	+++
GSL II	α- or β-GlcNAc	No	-	-
	α- or β-GlcNAc	Yes	-	-
Tomato lectin	(GlcNAc) ₂ to (GlcNAc) ₄	No	+/-	+/-

^a Cells, with or without pretreatment with neuraminidase, were incubated with WGA, ricin, concanavalin A, *Griffonia simplicifolia* lectin II (GSL II), and tomato lectin. The degrees of cell agglutination, from none (-) to completely (+++) agglutinated, were scored by light microscopy. Similar results were obtained when lectins were used at 0.1, 1, 2.5, and 10 μg/ml. Control cells without lectin were always viable and nonagglutinated.

To confirm that the [³H]mannose label in the high-MW glycoconjugate fraction seen in Fig. 3C was associated with ricin-binding glycoproteins (see below), we also performed a pull-down from the [³H]mannose-labeled TbGPI12 null mutant total cell lysate with ricin-agarose. Subsequent SDS-PAGE and fluorography revealed that the radiolabeled material pulled down by the ricin lectin contained the high-MW glycoconjugate (Fig. 3D, lane 7).

In a separate experiment, TbGPI12 null cells labeled with [³H]mannose were extracted overnight with chloroform-methanol water (1:2:0.8, vol/vol), and the insoluble pellet extracted with 9% butan-1-ol in water. The latter fraction and the final pellet solubilized in SDS-sample buffer were analyzed by SDS-PAGE and fluorography. No radiolabeled products were found in the 9% butan-1-ol extract, whereas several labeled bands were observed in the final pellet solubilized in SDS-sample buffer (data not shown), indicating that, like wild-type procyclic-form cells, the TbGPI12 null mutant cells do not express any lipophosphoglycan-like molecules (9).

Cell agglutination with lectins. To provide direct evidence for the exposure of carbohydrates on the surface, live wild-type and procyclin-less TbGPI12 null cells were washed and assayed for agglutination by various lectins (Table 2). Wheat germ agglutinin (WGA) and concanavalin A both agglutinated wild-type and TbGPI12 null cells and, at higher concentrations, caused cell death. However, ricin (RCA120) had no effect on either cell type unless they were pretreated with *Clostridium perfringens* neuraminidase, after which it caused efficient agglutination but not cell death. The WGA lectin has dual specificity and recognizes both terminal sialic acid and GlcNAc residues. In this case, WGA only agglutinated cells before treatment with neuraminidase. Furthermore, the terminal GlcNAc-specific *Griffonia simplicifolia* lectin II failed to agglutinate the cells before or after neuraminidase treatment. Taken together, these results suggest that both wild-type and TbGPI12 null cells express terminal sialic acid residues linked

to underlying galactose residues on their cell surface. The absence of significant agglutination by tomato lectin suggests an absence of surface-linear poly-*N*-acetylglucosamine structures.

Surface labeling with galactose oxidase-sodium borotritide. To check that the high-MW glycoconjugate(s) contains subterminal galactose residues by an independent method, and to assess the accessibility of those galactose residues on the high-MW glycoconjugate(s) in the presence and absence of the procyclin coat, we performed cell surface labeling of *C. perfringens* neuraminidase treated with live wild-type and TbGPI12 null cells by the galactose oxidase-NaB[³H]₄ method (10). A slight modification of the standard method was developed in these studies, namely, the prereluction of the living cells with nonradioactive 1 mM NaBH₄ under physiological conditions prior to washing and galactose oxidase-NaB[³H]₄ labeling. We found that this modification greatly reduced non-specific radiolabeling, and we would recommend it to others planning to use this cell surface-labeling method.

Using this method, the procyclins, as well as the free GPIs, of wild-type cells were labeled after (but not before) galactose oxidase treatment (Fig. 4, lanes 1 and 2), consistent with their known structures (reviewed in reference 14). However, the high-MW glycoconjugates were even more efficiently labeled than the procyclins (Fig. 4, lane 1), suggesting that they contain significantly more terminal galactose residues (after neuraminidase treatment) than the procyclins and/or that they are preferentially reactive with galactose oxidase. Most significantly, the labeling of the high-MW glycoconjugate(s) was the same in the wild-type cells and in the TbGPI12 null mutants (Fig. 4, compare lanes 1 and 3), suggesting that on live cells, the procyclin coat has no effect on the accessibility of the 68-kDa galactose oxidase enzyme to the high-MW glycoconjugate(s).

Together with the lectin data, the surface labeling results support a model in which the high-MW glycoconjugate(s) terminate in sialic acid-galactose motifs in both wild-type and

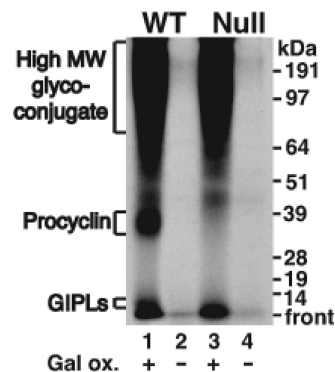


FIG. 4. Cell surface labeling of the high-apparent-MW glycoconjugate fraction on neuraminidase-treated wild-type (WT) and TbGPI12 null (Null) procyclic cells with galactose oxidase and NaB[³H]₄. The wild-type (lanes 1 and 2) and TbGPI12 null (lanes 3 and 4) procyclic cells were treated (+) or not treated (-) with galactose oxidase (Gal ox.), as indicated, prior to reduction with NaB[³H]₄. After washing, the cells were lysed and analyzed by SDS-PAGE and fluorography. The positions of the MW markers are shown on the right. GPIs, free GPIs, or glycoinositolphospholipids.

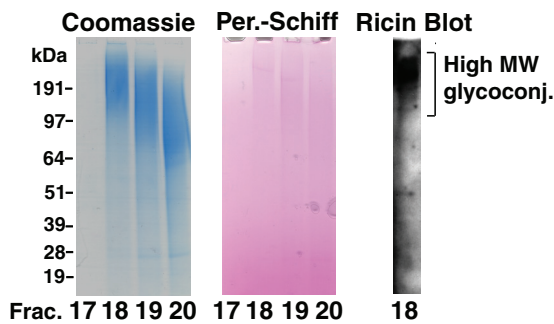


FIG. 5. Purification of the high-MW glycoconjugate fraction. After ricin affinity chromatography, the majority of the high-MW glycoconjugate fraction was eluted in fractions 18 to 20 from a Superose 6B gel filtration column. Aliquots of fractions 17 to 20, corresponding to molecules with a predicted molecular mass of 6 MDa to 600 kDa, were analyzed by SDS-PAGE and stained for protein with Coomassie blue or for carbohydrate by periodate-Schiff (Per.-Schiff). A sample of fraction 18 was also subjected to ricin blotting. The positions of the MW markers are shown on the left.

TbGPI12 null cells and that these molecules coexist with procyclins and free GPIs in the wild-type cells.

Purification of the high-MW glycoconjugates by ricin affinity chromatography and gel filtration. TbGPI12 null cells from 5 liters of culture were extensively washed in PBS under conditions that allow the complete removal of cell surface sialic acid through the combined activities of endogenous cell surface neuraminidase and *trans*-sialidase (the latter works as an α 2- and α 3-specific neuraminidase in the absence of serum sialyl donor glycoproteins). The cells were then subjected to hypotonic lysis, and the washed cell ghosts were solubilized with an SDS, urea and DTT-containing buffer. The clarified lysate was diluted with *n*-octylglucoside buffer and applied to ricin-agarose beads as described previously (3). The beads were washed extensively to remove nonspecifically bound proteins and eluted first with lactose and galactose and second with 1% SDS to recover all adsorbed material. The combined eluates were concentrated and applied to a Superose 6 gel filtration column equilibrated in buffer containing 0.1% SDS and 10 mM DTT. Fractions 18 to 20 (corresponding to proteins with a molecular mass of >600 kDa) were subjected to SDS-PAGE and shown to contain high-MW glycoconjugate(s) that could be stained for protein with colloidal Coomassie blue and for carbohydrate with periodate-Schiff and, after transfer to nitrocellulose, could be blotted with ricin (Fig. 5). If 30 mg/ml galactose and lactose were added prior to ricin-agarose pulldown, no comparable material was isolated (data not shown).

Carbohydrate composition of the high-MW glycoconjugate fraction. Aliquots of pooled fractions 18 to 20 from the Superose 6 fractionation were subjected to protein quantification and to quantitative carbohydrate composition analysis by GC-MS (Table 3). From these data, we estimate that about 7% of the fraction is carbohydrate, by mass. The monosaccharides present are mannose, galactose, and *N*-acetylglucosamine (typical of *T. brucei* glycoproteins) and fucose. Fucose has not been previously described in any glycoconjugate of *T. brucei*.

Characterization of components of the high-MW glycoconjugate fraction. The colloidal Coomassie blue-stained smear in

fraction 18 (Fig. 5) was excised from the gel, digested with trypsin, and submitted to LC-MS/MS for proteomic identification (Table 4). The majority of the hits were putative integral membrane proteins that span the bilayer several times, and the putative single-pass transmembrane procyclic-form specific antigen PSSA-2 (15) was noticeably absent (see Discussion). Some of the identified multispreading membrane protein hits are known or assumed to be plasma membrane proteins, like the TbN10 nucleoside transporter (46), the THT2A glucose transporter (4), and the recently described TbPAD2 putative carboxylate transporter (6). To validate other hits as surface molecules, we acquired available antibodies to two components, P-type ATPase and VHPPase. The antibody to the P-type ATPase was raised against a *T. cruzi* sequence that has 80% identity and good immunological cross-reactivity to the *T. brucei* homologue (21, 22). Fraction 18 from the Superose 6 fractionation was tested by Western blotting with antiproton ATPase (Fig. 6A). A band with an apparent MW similar to that predicted for the *T. brucei* P-type ATPase was observed (at about 100 kDa) together with a >200-kDa smear. A similar pattern of staining has been reported previously for this protein (21). We used the same antibodies to localize the *T. brucei* P-type ATPase in fixed and permeabilized wild-type and TbGPI12 null cells by immunofluorescence microscopy (Fig. 7A). In both cases, a strong cell surface label was apparent, in agreement with the results presented in reference 21.

Antibodies raised to a recombinant segment of the *T. brucei* VHPPase (18) also recognized a high-MW smear in fraction 18 from the Superose 6 fractionation (Fig. 6B). These same antibodies, and two anti-synthetic peptide antibodies made for regions of plant VHPPase that have almost complete sequence identity with the *T. brucei* homologue (41), were used to label live cells and fixed and permeabilized cells. As expected, the former showed intense staining of intracellular structures (data not shown), consistent with previous reports of its localization in acidocalcisomes (18). However, the antibodies also labeled discrete cell surface patches on intact, live wild-type and TbGPI12 null cells (Fig. 7B). The appearance of the VHPPase in discrete patches on the surface of live parasites may be due to capping induced by the antibodies prior to fixation. The localization of VHPPase to both the plasma membrane and the acidocalcisome has been previously reported for *T. cruzi* (24, 43).

TABLE 3. Monosaccharide composition of the high-MW glycoconjugate fraction^a

Monosaccharide ^b	Amt of protein (nmol/mg) ^c	% by wt
Mannose	175 ± 25	2.8
Galactose	162 ± 19	2.6
Fucose	83 ± 16	1.2
<i>N</i> -Acetylglucosamine	Present but not quantitated ^d	N/A ^e

^a Pooled material (fractions 18 to 20) from the gel filtration step of the purification was analyzed for protein content by colorimetric assay and monosaccharide content by GC-MS.

^b Glucose and a trace of xylose were also detected, but these are common contaminants of biological preparations and have been omitted from the table.

^c Means and standard deviations of the results from triplicate analyses.

^d The *N*-acetylglucosamine derivatives were positively identified by retention time and mass spectrum, but quantification of these derivatives is unreliable.

^e N/A, not applicable.

TABLE 4. Proteins identified in the high-MW glycoconjugate fraction^a

Protein	Gene no.	Mascot score ^c	No. of matched peptides	Molecular mass (kDa) ^d	No. of transmembrane domains ^e	No. of N-glycosylation sites ^f
<i>Tubulin</i> ^b	<i>Tb927.1.2330</i>	1171	38	50	0	N/A
VHPPase	Tb927.4.4380	812	22	86	14	3
Hypothetical protein	Tb927.4.2530	640	13	17	4	1
TbPAD2, putative carboxylate transporter	Tb927.7.5940 ^g	435	18	67	14	2
<i>Triosephosphate-isomerase</i>	<i>Tb11.02.3210</i>	297	6	27	0	N/A
P-type proton-ATPase (TbHA1 and/or TbHA2)	Tb10.389.1180 and/or Tb10.389.1170	269	11	100	7	1
Adenosine nucleoside transporter (P1); TbNT10	Tb09.160.5480	213	6	51	10	1
Oxoglutarate-malate carrier protein	Tb10.389.0690	210	6	33	4	1
Copper-transporting ATPase-like protein	Tb11.47.0023	197	4	102	10	5
ADP-ATP translocase protein	Tb10.61.1830	187	9	34	3	2
PGPA multidrug resistance protein A	Tb927.8.2160	171	7	175	11	7
Glucose transporter (THT2A)	Tb10.6k15.2020	169	3	57	12	2
PGPA multidrug resistance protein E	Tb927.4.4490	163	5	194	8	9

^a Proteins identified by LC-MS/MS in fraction 18 by gel filtration of the high-MW glycoconjugate fraction. N/A, not applicable.

^b Proteins in italics are major cytosolic proteins that are unlikely to be glycosylated and are most likely contaminants.

^c The proteins are ordered by Mascot score, which to a first approximation, tends to correlate with relative protein abundance.

^d Predicted molecular mass from the predicted coding sequence.

^e Number of predicted transmembrane domains according to TMHMM2 (16).

^f Number of predicted N-glycosylation sites according to NetNGlyc.

^g Tb927.7.5940 belongs to a family of eight closely related sequences. However, three peptides unique to Tb927.7.5490 were observed (TFTGLGAAIVGSIQLAF FSK, LCMGYFEVWSQK, and AEDRVPIITLSMFVPSVCIITMLTLFLTLPK), suggesting that this is the main form of the family detected in this experiment.

Attempts to observe the localization of VHPPase by immunoelectron microscopy were not successful. However, to further analyze the cell surface P-type ATPase, live wild-type and TbGPI12 null cells were incubated with rabbit anti-P-type ATPase, washed, fixed with paraformaldehyde, and then labeled by incubation with protein A conjugated to 10-nm gold particles. Specific and similar densities of the cell surface labeling of P-type ATPase were seen for both cell types (Fig. 8).

DISCUSSION

We previously described the lack of procyclins on the surface of the *T. brucei* procyclic-form TbGPI12 null mutant (11). Here, we have more thoroughly monitored the fate of the procyclin protein in these cells. The absence of a GPI anchor does not appear to affect the processing of the single N-glycosylation sequon in EP procyclins in the ER, such that all cell-associated and secreted procyclin fragments appear

to be N-glycosylated, like wild-type procyclin, with endo H-sensitive oligomannose glycans. Further, since the antibody used to precipitate the procyclin fragments recognizes the EP repeat domain that is immediately preceded by the N-glycosylation site, we suggest that the majority of the procyclin fragments found in the cells and the supernatant are generated by the proteolysis of the N-terminal domain of the procyclin molecules. In summary, in the absence of a GPI anchor addition, the procyclins appear to be normally N-glycosylated in the ER, transported to the lysosomal compartment, proteolytically degraded in the N-terminal domain, and secreted from the cells into the culture supernatant. The appearance of proteolytically degraded procyclin in the culture supernatant of TbGPI10 null mutants has also been described (30). These data suggest that proteins can traffic from the lysosome to the surrounding medium in procyclic-form *T. brucei*, presumably via the flagellar pocket. We also noted the shedding of fully processed wild-type procyclin into the culture supernatant of procyclic cells. However, the amount of shedding was low and the slow release of GPI-anchored proteins containing two acyl chains from the surface of *T. brucei* has been previously noted (42).

The ability to radiolabel a high-MW glycoconjugate fraction with glucosamine, mannose, and glucose (though mannose can be metabolized into fucose, and glucose can be metabolized into several other sugars by trypanosomes [52]) is consistent with the ability to agglutinate both wild-type and surface procyclin-less TbGPI12 null mutant cells with lectins. The pattern of lectin agglutination (i.e., agglutination by WGA only prior to desialylation and by ricin only after desialylation) is consistent with the presence of glycans that terminate in galactose residues capped with sialic acid. This model is consistent with the ability to surface label the high-MW material of desialylated parasites using galactose oxidase and NaB[³H]₄ reduc-

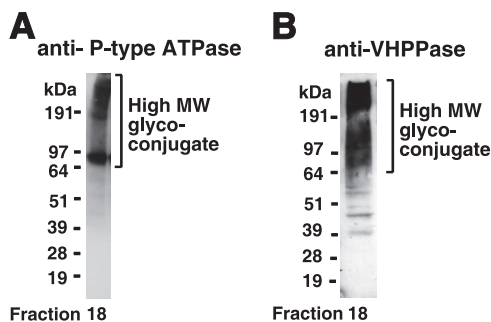


FIG. 6. Identification of P-type ATPase and VHPPase in the high-MW glycoconjugate fraction. (A) Western blot of fraction 18 from gel filtration with anti-P-type ATPase antibodies. (B) Western blot of fraction 18 from gel filtration with anti-VHPPase antibodies.

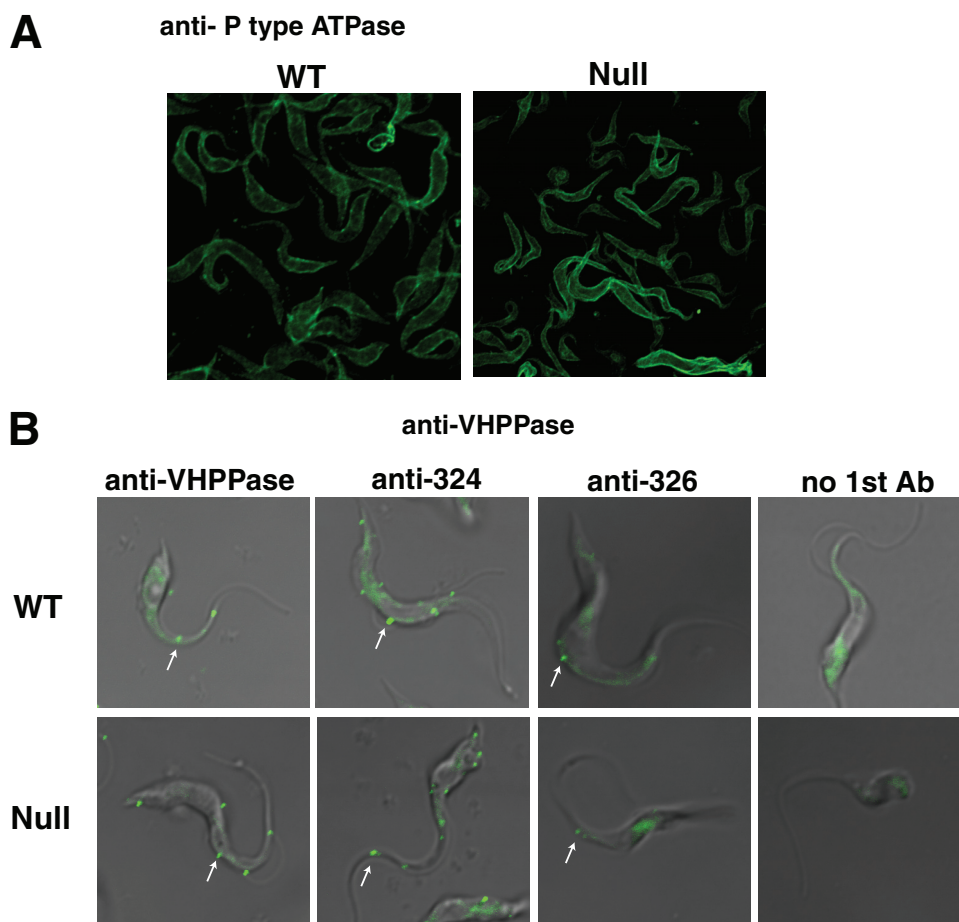


FIG. 7. Localization of P-type ATPase and VHPPase in wild-type and TbGPI12 null procyclic cells by immunofluorescence microscopy. (A) Fixed and permeabilized cells were stained with rabbit anti-P-type ATPase antibodies followed by fluorescently labeled secondary antibodies, revealing cell surface labeling in both cases. (B) Live cells were incubated with no primary antibody (no 1st Ab; right panels), antibodies raised to a fragment of recombinant VHPPase antibodies (left panels), or one of two anti-VHPPase synthetic peptide antibodies (middle panels); fixed; and then stained with fluorescently labeled secondary antibodies. Punctate staining of surface structures is indicated by white arrows.

tion. Significantly, the galactose oxidase- $\text{NaB}[\text{}^3\text{H}]_4$ labeling of the high-MW glycoconjugate(s) on living procyclic cells was unaffected by the presence (in wild-type cells) or absence (in TbGPI12 null mutants) of the GPI-anchored procyclin coat. Similarly, we found that the presence or absence of the procyclins had no effect on our ability to label cell surface P-type ATPase molecules on live cells with specific antibodies. These data strongly suggest that the procyclin coat does not prevent the approach of proteins of 68 kDa (galactose oxidase) or 150 kDa (immunoglobulin G) to non-GPI-anchored cell surface coat components on live cells.

Ricin affinity purification of the high-MW glycoconjugate was performed from the TbGPI12 null cells, thus obviating the need to purify it away from the procyclins and free GPIs present in the wild-type cells. Compositional analysis confirmed the glycoprotein nature of this material, and the presence of galactose is consistent with ricin binding. Fucose was also found in the preparation. This sugar has been found previously in gp72 of *T. cruzi* (8, 12), a homologue of the *T. brucei* Fla-1 and Fla-2 flagellar adhesion zone glycoproteins (17, 31), but has not been previously reported in any *T. brucei* glycoconjugate. However, the sugar nucleotide

GDP-fucose was recently identified in bloodstream and procyclic-form *T. brucei* and shown to be essential for both life cycle stages (52, 53).

The proteomic analysis of the high-MW glycoconjugate revealed multiple known and putative multispinning transmembrane proteins with a variety of predicted monomeric molecular masses, ranging from 17 to 194 kDa. The elution of this material by gel filtration, in the presence of SDS, in fractions predicted to contain molecules in excess of 600 kDa and the appearance of this material on SDS-PAGE as a smear ranging from 65 kDa to the top of the gel suggest an unusual physical state. However, multispinning membrane proteins can undergo aggregation under denaturing conditions (40, 45). We therefore checked to see whether the appearance by SDS-PAGE of the galactose oxidase- $\text{NaB}[\text{}^3\text{H}]_4$ -labeled high-MW glycoconjugate(s) changes when we extracted the cells at 100°C, 50°C, or 37°C and whether or not the presence of 4 M urea had any effect (see Fig. S2 in the supplemental material). The results indicate that, in the absence of urea, temperature has no effect on the extraction efficiency or appearance of the labeled products on SDS-PAGE, whereas lower temperatures were less efficient in the presence of urea, and that at 100°C, 4

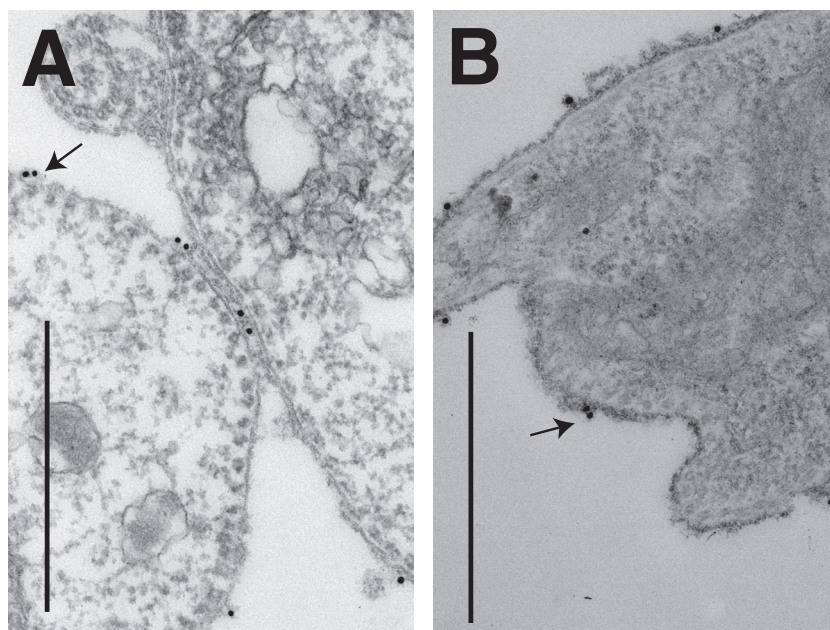


FIG. 8. Localization of P-type ATPase on live wild-type and TbGPI12 null procyclic cells by immunoelectron microscopy. Live wild-type (A) and TbGPI12 null (B) cells were labeled with rabbit anti-P-type ATPase antibodies and fixed. Anti-P-type ATPase antibodies were revealed with 10-nm gold particles conjugated to protein A. The images were magnified $\times 26,000$, and the black bars correspond to 1 μm in panels A and B. Black arrows indicate representative sites of surface labeling.

M urea assisted in the dissociation of the very high-apparent-MW material that ran at the top of the gel into material that entered the gel. We conclude that the appearance of the high-MW glycoconjugate material on the SDS-PAGE gels is due in part to glycosylation but that cross-linking and/or temperature- and urea-insensitive aggregation of the components may also be a factor. It may be significant that no single-pass transmembrane proteins, like PSSA-2 (15), were identified in the high-MW glycoconjugate fraction, suggesting that these might not be modified with ricin-binding glycans and/or do not coaggregate with the aforementioned multispansing membrane proteins.

The presence of *N*-acetylglucosamine and mannose in the sugar composition of the high-MW glycoconjugate material is suggestive of protein *N*-glycosylation. However, despite numerous attempts, we were unable to show convincing effects using PNGase F to de-*N*-glycosylate the glycoproteins. This could be due to difficulties in the enzyme reaching the glycosylation sites because of an unusual cross-linked/aggregated physical state and/or the presence of $\alpha 1$ - to $\alpha 3$ -linked fucose attached to the chitobiosyl core of the glycans, which is known to render *N*-glycans resistant to PNGase F (49). In addition, it is possible that the material contains *O*-linked oligosaccharides, as found in *T. cruzi* mucins (35, 44), and/or phosphate-linked oligosaccharides, as found in leishmania (13), *T. cruzi* (12, 23), and *Trypanosoma congolense* (48). A detailed analysis of the carbohydrate moieties in the high-MW glycoconjugate fraction will be undertaken but is beyond the scope of this report.

Taking two examples of the transmembrane proteins purified by ricin affinity chromatography for which antibody reagents are available, the P-type ATPase and the VHP-

Pase, we were able to confirm previous reports that the P-type ATPase is expressed on the surface of procyclic-form *T. brucei* cells (22) and that, like in *T. cruzi* (43), VHPase is present both in the plasma and the membrane of the acidocalcisome in procyclic-form *T. brucei*. The presence of VHPase in these two locations suggests that the biogenesis of the plasma membrane and acidocalcisome membrane may share common origins.

In summary, the high-MW glycoconjugate and residual surface coat of procyclic-form *T. brucei*, identified by deleting all surface GPI-anchored molecules in the TbGPI12 null mutant (11), appears to be made up predominantly of multispansing transmembrane proteins, several of which are proton and nutrient transporters. These appear to be significantly glycosylated with galactose, mannose, *N*-acetylglucosamine, and fucose-containing glycans that normally terminate with sialic acid linked to galactose. We suggest that this group of transporters, and possibly other as-yet-unidentified molecules, exists alongside the procyclins in wild-type cells and that this network of molecules is not sterically protected from the approach of macromolecules by the procyclin coat. On the other hand, the combination of the procyclin coat and the glycosylated transporter-containing molecules may well play a physical role in protecting the plasma membrane, as well as a role in maintaining intracellular pH and transporting nutrients and terminal metabolites.

ACKNOWLEDGMENTS

This work was supported by a Wellcome Trust program grant to M.A.J.F. (085622) and a Wellcome Trust strategic award (083481).

We thank Roberto Docampo, Philip Rea, Norbert Bakalara, and Jay Bangs for kindly providing antibodies and Alvaro Acosta Serrano for helpful discussions.

REFERENCES

- Acosta-Serrano, A., R. N. Cole, A. Mehlert, M. G. Lee, M. A. Ferguson, and P. T. Englund. 1999. The procyclin repertoire of *Trypanosoma brucei*. Identification and structural characterization of the Glu-Pro-rich polypeptides. *J. Biol. Chem.* **274**:29763–29771.
- Acosta-Serrano, A., E. Vassella, M. Liniger, C. Kunz Renggli, R. Brun, I. Roditi, and P. T. Englund. 2001. The surface coat of procyclic *Trypanosoma brucei*: programmed expression and proteolytic cleavage of procyclin in the tsetse fly. *Proc. Natl. Acad. Sci. USA* **98**:1513–1518.
- Atrih, A., J. M. Richardson, A. R. Prescott, and M. A. Ferguson. 2005. *Trypanosoma brucei* glycoproteins contain novel giant poly-N-acetylglucosamine carbohydrate chains. *J. Biol. Chem.* **280**:865–871.
- Bringaud, F., and T. Baltz. 1993. Differential regulation of two distinct families of glucose transporter genes in *Trypanosoma brucei*. *Mol. Cell. Biol.* **13**:1146–1154.
- Brun, R., and Schonberger. 1979. Cultivation and in vitro cloning of procyclic culture forms of *Trypanosoma brucei* in a semi-defined medium. Short communication. *Acta Trop.* **36**:289–292.
- Dean, S., R. Marchetti, K. Kirk, and K. R. Matthews. 2009. A surface transporter family conveys the trypanosome differentiation signal. *Nature* **459**:213–217.
- Engstler, M., G. Reuter, and R. Schauer. 1993. The developmentally regulated trans-sialidase from *Trypanosoma brucei* sialylates the procyclic acidic repetitive protein. *Mol. Biochem. Parasitol.* **61**:1–13.
- Ferguson, M. A., A. K. Allen, and D. Snary. 1983. Studies on the structure of a phosphoglycoprotein from the parasitic protozoan *Trypanosoma cruzi*. *Biochem. J.* **213**:313–319.
- Ferguson, M. A., P. Murray, H. Rutherford, and M. J. McConville. 1993. A simple purification of procyclic acidic repetitive protein and demonstration of a sialylated glycosyl-phosphatidylinositol membrane anchor. *Biochem. J.* **291**:51–55.
- Gahmberg, C. G., and S. I. Hakomori. 1973. External labeling of cell surface galactose and galactosamine in glycolipid and glycoprotein of human erythrocytes. *J. Biol. Chem.* **248**:4311–4317.
- Guther, M. L., S. Lee, L. Tetley, A. Acosta-Serrano, and M. A. Ferguson. 2006. GPI-anchored proteins and free GPI glycolipids of procyclic form *Trypanosoma brucei* are nonessential for growth, are required for colonization of the tsetse fly, and are not the only components of the surface coat. *Mol. Biol. Cell* **17**:5265–5274.
- Haynes, P. A., M. A. Ferguson, and G. A. Cross. 1996. Structural characterization of novel oligosaccharides of cell-surface glycoproteins of *Trypanosoma cruzi*. *Glycobiology* **6**:869–878.
- Ilg, T., P. Overath, M. A. Ferguson, T. Rutherford, D. G. Campbell, and M. J. McConville. 1994. O- and N-glycosylation of the *Leishmania mexicana* secreted acid phosphatase. Characterization of a new class of phosphoserine-linked glycans. *J. Biol. Chem.* **269**:24073–24081.
- Izquierdo, L., M. Nakanishi, A. Mehlert, G. Machray, G. J. Barton, and M. A. Ferguson. 2009. Identification of a glycosylphosphatidylinositol anchor-modifying beta1-3 N-acetylglucosaminyl transferase in *Trypanosoma brucei*. *Mol. Microbiol.* **71**:478–491.
- Jackson, D. G., D. K. Smith, C. Luo, and J. F. Elliott. 1993. Cloning of a novel surface antigen from the insect stages of *Trypanosoma brucei* by expression in COS cells. *J. Biol. Chem.* **268**:1894–1900.
- Krogh, A., B. Larsson, G. von Heijne, and E. L. Sonnhammer. 2001. Predicting transmembrane protein topology with a hidden Markov model: application to complete genomes. *J. Mol. Biol.* **305**:567–580.
- LaCount, D. J., B. Barrett, and J. E. Donelson. 2002. *Trypanosoma brucei* FLA1 is required for flagellum attachment and cytokinesis. *J. Biol. Chem.* **277**:17580–17588.
- Lemercier, G., S. Dutoya, S. Luo, F. A. Ruiz, C. O. Rodrigues, T. Baltz, R. Docampo, and N. Bakalara. 2002. A vacuolar-type H⁺-pyrophosphatase governs maintenance of functional acidocalcisomes and growth of the insect and mammalian forms of *Trypanosoma brucei*. *J. Biol. Chem.* **277**:37369–37376.
- Lillico, S., M. C. Field, P. Blundell, G. H. Coombs, and J. C. Mottram. 2003. Essential roles for GPI-anchored proteins in African trypanosomes revealed using mutants deficient in GPI8. *Mol. Biol. Cell* **14**:1182–1194.
- Liniger, M., S. Urwyler, E. Studer, M. Oberle, C. K. Renggli, and I. Roditi. 2004. Role of the N-terminal domains of EP and GPEET procyclins in membrane targeting and the establishment of midgut infections by *Trypanosoma brucei*. *Mol. Biochem. Parasitol.* **137**:247–251.
- Luo, S., J. Fang, and R. Docampo. 2006. Molecular characterization of *Trypanosoma brucei* P-type H⁺-ATPases. *J. Biol. Chem.* **281**:21963–21973.
- Luo, S., D. A. Scott, and R. Docampo. 2002. *Trypanosoma cruzi* H⁺-ATPase 1 (TcHA1) and 2 (TcHA2) genes complement yeast mutants defective in H⁺ pumps and encode plasma membrane P-type H⁺-ATPases with different enzymatic properties. *J. Biol. Chem.* **277**:44497–44506.
- Macrae, J. I., A. Acosta-Serrano, N. A. Morrice, A. Mehlert, and M. A. Ferguson. 2005. Structural characterization of NETNES, a novel glycoconjugate in *Trypanosoma cruzi* epimastigotes. *J. Biol. Chem.* **280**:12201–12211.
- Martinez, R., Y. Wang, G. Benaim, M. Benchimol, W. de Souza, D. A. Scott, and R. Docampo. 2002. A proton pumping pyrophosphatase in the Golgi apparatus and plasma membrane vesicles of *Trypanosoma cruzi*. *Mol. Biochem. Parasitol.* **120**:205–213.
- Mehlert, A., A. Treumann, and M. A. Ferguson. 1999. *Trypanosoma brucei* GPEET-PARP is phosphorylated on six out of seven threonine residues. *Mol. Biochem. Parasitol.* **98**:291–296.
- Montagna, G., M. L. Cremona, G. Paris, M. F. Amaya, A. Buschiazzi, P. M. Alzari, and A. C. Frasch. 2002. The trans-sialidase from the African trypanosome *Trypanosoma brucei*. *Eur. J. Biochem.* **269**:2941–2950.
- Morris, J. C., Z. Wang, M. E. Drew, and P. T. Englund. 2002. Glycolysis modulates trypanosome glycoprotein expression as revealed by an RNAi library. *EMBO J.* **21**:4429–4438.
- Mowatt, M. R., and C. E. Clayton. 1987. Developmental regulation of a novel repetitive protein of *Trypanosoma brucei*. *Mol. Cell. Biol.* **7**:2838–2844.
- Nagamune, K., A. Acosta-Serrano, H. Uemura, R. Brun, C. Kunz-Renggli, Y. Maeda, M. A. Ferguson, and T. Kinoshita. 2004. Surface sialic acids taken from the host allow trypanosome survival in tsetse fly vectors. *J. Exp. Med.* **199**:1445–1450.
- Nagamune, K., T. Nozaki, Y. Maeda, K. Ohishi, T. Fukuma, T. Hara, R. T. Schwarz, C. Sutterlin, R. Brun, H. Riezman, and T. Kinoshita. 2000. Critical roles of glycosylphosphatidylinositol for *Trypanosoma brucei*. *Proc. Natl. Acad. Sci. USA* **97**:10336–10341.
- Nozaki, T., P. A. Haynes, and G. A. Cross. 1996. Characterization of the *Trypanosoma brucei* homologue of a *Trypanosoma cruzi* flagellum-adhesion glycoprotein. *Mol. Biochem. Parasitol.* **82**:245–255.
- Pays, E., L. Vanhamme, and D. Perez-Morga. 2004. Antigenic variation in *Trypanosoma brucei*: facts, challenges and mysteries. *Curr. Opin. Microbiol.* **7**:369–374.
- Peck, R. F., A. M. Shiflett, K. J. Schwartz, A. McCann, S. L. Hajduk, and J. D. Bangs. 2008. The LAMP-like protein p67 plays an essential role in the lysosome of African trypanosomes. *Mol. Microbiol.* **68**:933–946.
- Pontes de Carvalho, L. C., S. Tomlinson, F. Vandekerckhove, E. J. Bienen, A. B. Clarkson, M. S. Jiang, G. W. Hart, and V. Nussenzweig. 1993. Characterization of a novel trans-sialidase of *Trypanosoma brucei* procyclic trypanomastigotes and identification of procyclin as the main sialic acid acceptor. *J. Exp. Med.* **177**:465–474.
- Previato, J. O., C. Jones, L. P. Goncalves, R. Wait, L. R. Travassos, and L. Mendonca-Previato. 1994. O-glycosidically linked N-acetylglucosamine-bound oligosaccharides from glycoproteins of *Trypanosoma cruzi*. *Biochem. J.* **301**:151–159.
- Richardson, J. P., R. P. Beecroft, D. L. Tolson, M. K. Liu, and T. W. Pearson. 1988. Procyclin: an unusual immunodominant glycoprotein surface antigen from the procyclic stage of African trypanosomes. *Mol. Biochem. Parasitol.* **31**:203–216.
- Roditi, I., M. Carrington, and M. Turner. 1987. Expression of a polypeptide containing a dipeptide repeat is confined to the insect stage of *Trypanosoma brucei*. *Nature* **325**:272–274.
- Roditi, I., H. Schwarz, T. W. Pearson, R. P. Beecroft, M. K. Liu, J. P. Richardson, H. J. Buhning, J. Pleiss, R. Bulow, R. O. Williams, et al. 1989. Procyclin gene expression and loss of the variant surface glycoprotein during differentiation of *Trypanosoma brucei*. *J. Cell Biol.* **108**:737–746.
- Roper, J. R., M. L. Guther, J. I. Macrae, A. R. Prescott, I. Hallyburton, A. Acosta-Serrano, and M. A. Ferguson. 2005. The suppression of galactose metabolism in procyclic form *Trypanosoma brucei* causes cessation of cell growth and alters procyclin glycoprotein structure and copy number. *J. Biol. Chem.* **280**:19728–19736.
- Sagne, C., M. F. Isambert, J. P. Henry, and B. Gasnier. 1996. SDS-resistant aggregation of membrane proteins: application to the purification of the vesicular monoamine transporter. *Biochem. J.* **316**:825–831.
- Sarafian, V., Y. Kim, R. J. Poole, and P. A. Rea. 1992. Molecular cloning and sequence of cDNA encoding the pyrophosphate-energized vacuolar membrane proton pump of *Arabidopsis thaliana*. *Proc. Natl. Acad. Sci. USA* **89**:1775–1779.
- Schwartz, K. J., R. F. Peck, N. N. Tazeh, and J. D. Bangs. 2005. GPI valence and the fate of secretory membrane proteins in African trypanosomes. *J. Cell Sci.* **118**:5499–5511.
- Scott, D. A., W. de Souza, M. Benchimol, L. Zhong, H. G. Lu, S. N. Moreno, and R. Docampo. 1998. Presence of a plant-like proton-pumping pyrophosphatase in acidocalcisomes of *Trypanosoma cruzi*. *J. Biol. Chem.* **273**:22151–22158.
- Serrano, A. A., S. Schenkman, N. Yoshida, A. Mehlert, J. M. Richardson, and M. A. Ferguson. 1995. The lipid structure of the glycosylphosphatidylinositol-anchored mucin-like sialic acid acceptors of *Trypanosoma cruzi* changes during parasite differentiation from epimastigotes to infective metacyclic trypomastigote forms. *J. Biol. Chem.* **270**:27244–27253.
- Soulie, S., J. V. Moller, P. Falson, and M. le Maire. 1996. Urea reduces the

- aggregation of membrane proteins on sodium dodecyl sulfate-polyacrylamide gel electrophoresis. *Anal. Biochem.* **236**:363–364.
46. **Spoerri, I., R. Chadwick, C. K. Renggli, K. Matthews, I. Roditi, and G. Burkard.** 2007. Role of the stage-regulated nucleoside transporter TbNT10 in differentiation and adenosine uptake in *Trypanosoma brucei*. *Mol. Biochem. Parasitol.* **154**:110–114.
 47. **Taylor, J. E., and G. Rudenko.** 2006. Switching trypanosome coats: what's in the wardrobe? *Trends Genet.* **22**:614–620.
 48. **Thomson, L. M., D. J. Lamont, A. Mehlert, J. D. Barry, and M. A. Ferguson.** 2002. Partial structure of glutamic acid and alanine-rich protein, a major surface glycoprotein of the insect stages of *Trypanosoma congolense*. *J. Biol. Chem.* **277**:48899–48904.
 49. **Tretter, V., F. Altmann, and L. Marz.** 1991. Peptide-N4-(N-acetyl-beta-glucosaminyl)asparagine amidase F cannot release glycans with fucose attached alpha 1–3 to the asparagine-linked N-acetylglucosamine residue. *Eur. J. Biochem.* **199**:647–652.
 50. **Treumann, A., N. Zitzmann, A. Hulsmeier, A. R. Prescott, A. Almond, J. Sheehan, and M. A. Ferguson.** 1997. Structural characterisation of two forms of procyclic acidic repetitive protein expressed by procyclic forms of *Trypanosoma brucei*. *J. Mol. Biol.* **269**:529–547.
 51. **Triggs, V. P., and J. D. Bangs.** 2003. Glycosylphosphatidylinositol-dependent protein trafficking in bloodstream stage *Trypanosoma brucei*. *Eukaryot. Cell* **2**:76–83.
 52. **Turnock, D. C., and M. A. Ferguson.** 2007. Sugar nucleotide pools of *Trypanosoma brucei*, *Trypanosoma cruzi*, and *Leishmania major*. *Eukaryot. Cell* **6**:1450–1463.
 53. **Turnock, D. C., L. Izquierdo, and M. A. Ferguson.** 2007. The de novo synthesis of GDP-fucose is essential for flagellar adhesion and cell growth in *Trypanosoma brucei*. *J. Biol. Chem.* **282**:28853–28863.
 54. **Vassella, E., A. Acosta-Serrano, E. Studer, S. H. Lee, P. T. Englund, and I. Roditi.** 2001. Multiple procyclin isoforms are expressed differentially during the development of insect forms of *Trypanosoma brucei*. *J. Mol. Biol.* **312**:597–607.
 55. **Vassella, E., P. Butikofer, M. Engstler, J. Jelk, and I. Roditi.** 2003. Procyclin null mutants of *Trypanosoma brucei* express free glycosylphosphatidylinositols on their surface. *Mol. Biol. Cell* **14**:1308–1318.
 56. **Vassella, E., J. V. Den Abbeele, P. Butikofer, C. K. Renggli, A. Furger, R. Brun, and I. Roditi.** 2000. A major surface glycoprotein of *Trypanosoma brucei* is expressed transiently during development and can be regulated posttranscriptionally by glycerol or hypoxia. *Genes Dev.* **14**:615–626.
 57. **Vassella, E., M. Oberle, S. Urwyler, C. K. Renggli, E. Studer, A. Hemphill, C. Fragoso, P. Butikofer, R. Brun, and I. Roditi.** 2009. Major surface glycoproteins of insect forms of *Trypanosoma brucei* are not essential for cyclical transmission by tsetse. *PLoS ONE* **4**:e4493.